Published February 9, 2009

Kinetochore-generated pushing forces separate centrosomes during bipolar spindle assembly

Alberto Toso,[1] Jennifer R. Winter,[2] Ainslie J. Garrod,[2] Ana C. Amaro,[1] Patrick Meraldi,[1] and Andrew D. McAinsh[2]

[1]Institute of Biochemistry, ETH Zurich, CH-8093 Zurich, Switzerland
[2]Chromosome Segregation Laboratory, Marie Curie Research Institute, Oxted, Surrey RH8 0TL, England, UK

In animal somatic cells, bipolar spindle formation requires separation of the centrosome-based spindle poles. Centrosome separation relies on multiple pathways, including cortical forces and antiparallel microtubule (MT) sliding, which are two activities controlled by the protein kinase aurora A. We previously found that depletion of the human kinetochore protein Mcm21R^{CENP-O} results in monopolar spindles, raising the question as to whether kinetochores contribute to centrosome separation. In this study, we demonstrate that kinetochores promote centrosome separation after nuclear envelope breakdown by exerting a pushing force on the kinetochore fibers (k-fibers), which are bundles of MTs that connect kinetochores to centrosomes. This force is based on poleward MT flux, which incorporates new tubulin subunits at the plus ends of k-fibers and requires stable k-fibers to drive centrosomes apart. This kinetochore-dependent force becomes essential for centrosome separation if aurora A is inhibited. We conclude that two mechanisms control centrosome separation during prometaphase: an aurora A–dependent pathway and a kinetochore-dependent pathway that relies on k-fiber–generated pushing forces.

Introduction

To guarantee that the genomic information is faithfully transmitted during cell division, sister chromatids must be equally distributed to each daughter cell during chromosome segregation. In eukaryotic cells, this process requires the formation of a bipolar mitotic spindle. This structure is assembled from dynamic microtubules (MTs), which have their minus ends nucleated at the spindle poles and their plus ends extending outwards (Walczak and Heald, 2008). The MT plus ends make physical contact with the cell cortex and kinetochores, which are multiprotein structures that assemble on centromeric DNA. As sister kinetochores bind to kinetochore MTs (kinetochore fibers [k-fibers]) emanating from opposite poles, sister chromatids are segregated accurately during anaphase. A key challenge is to understand the mechanisms by which this coupled system of spindle poles, MTs, kinetochores, and cortical attachment sites cooperates to drive bipolar spindle assembly and chromosome segregation.

In most animal cells, bipolar spindle formation requires the separation of the duplicated centrosomes, which are the main MT-organizing centers that form the core of the two spindle poles. This separation event is driven by multiple pathways, such as cortical forces and antiparallel MT sliding, and is controlled by key mitotic kinases, such as aurora A and Polo-like kinase 1 (Barr et al., 2004; Barr and Gergely, 2007). Aurora A is thought to control cortical forces by regulating the growth of astral MTs and regulate MT sliding by phosphorylating the kinesin-5 Eg5 (Barr and Gergely, 2007). Although bipolar spindle formation can occur in the absence of centrosomes via chromatin-induced MT nucleation (the Ran pathway) and the self-organizing ability of MTs, the centrosomes, whenever present, exert a dominant effect on bipolar spindle formation (Heald et al., 1997). Several studies also showed that kinetochores or MT kinetochore attachment is not essential and can even hinder centrosome separation and bipolar spindle formation when centrosome function is impaired (Heald et al., 1996; Bucciarelli et al., 2003; Ganem and Compton, 2004).

However, a recent study showed that depletion of the human kinetochore protein Mcm21R (also known as centromere

A. Toso and J.R. Winter contributed equally to this paper.

Correspondence to Patrick Meraldi: patrick.meraldi@bc.biol.ethz.ch; or Andrew D. McAinsh: a.mcainsh@mcri.ac.uk

Abbreviations used in this paper: CENP-E, centromere protein E; hTERT, human telomerase reverse transcriptase; k-fiber, kinetochore fiber; MCAK, mitotic centromere-associated kinesin; mRFP, monomeric RFP; MT, microtubule; NEBD, nuclear envelope breakdown; PA, photoactivatable.

The Rockefeller University Press $30.00
J. Cell Biol. Vol. 184 No. 3 365–372
www.jcb.org/cgi/doi/10.1083/jcb.200809055

Supplemental Material can be found at:
http://jcb.rupress.org/cgi/content/full/jcb.200809055/DC1

Published February 9, 2009

protein O; Foltz et al., 2006) delays centrosome separation, resulting in 30–40% of mitotic cells containing monopolar spindles (McAinsh et al., 2006). However, the molecular mechanism by which Mcm21R-depleted kinetochores impair centrosome separation and whether this reflects a more general role for kinetochores in centrosome separation remains unknown. In this study, we investigate these questions by live cell imaging and siRNA-mediated protein depletion and find that kinetochores contribute to spindle bipolarity by using poleward MT flux to push centrosomes apart. This kinetochore-dependent spindle assembly pathway cooperates with aurora A, as inactivation of both poleward MT flux and aurora A inhibit bipolar spindle assembly in an additive manner.

Results and discussion

To evaluate how Mcm21R depletion affects centrosome separation, we monitored bipolar spindle formation using time-lapse microscopy in HeLa cells expressing histone 2B (H2B)–EGFP (to mark chromosomes) and α-tubulin–monomeric RFP (mRFP; to mark MTs). Inactivation of the spindle checkpoint and delayed bipolar spindle formation in Mcm21R-depleted cells led to monopolar anaphases (McAinsh et al., 2006). Strikingly, all cells that underwent a monopolar anaphase had unseparated centrosomes at nuclear envelope breakdown (NEBD; visible as the time point at which MTs penetrated the nuclear space) with centrosomes in close proximity on the same side of the nuclear membrane (Fig. 1 A). In contrast, cells with separated centrosomes at NEBD never underwent a monopolar anaphase (Fig. 1 A).

This suggested that the consequence of Mcm21R depletion depends on whether or not centrosome separation has occurred at NEBD. Previous studies suggested that vertebrate somatic cells do not synchronize centrosome separation and NEBD and described two pathways by which cells separate centrosomes: either by using the nuclear membrane during prophase (prophase pathway) or by using astral MT pulling forces and interactions between the two MT asters during prometaphase (prometaphase pathway; for review see Rosenblatt, 2005). Fixed and live cell imaging indicated that 52% of HeLa cells used the prophase pathway, whereas 48% used the prometaphase pathway (Fig. 1, B and C; and Video 1, available at http://www.jcb.org/cgi/content/full/jcb.200809055/DC1). These two pathways were not an artifact of transformed cells, as untransformed human telomerase reverse transcriptase (hTERT)–RPE1 (retinal pigment epithelial) cells used both pathways to the same extent (Fig. S1 A). Importantly, siRNA-mediated depletion of the intracentrosome linkage protein rootletin, which induces premature centrosome splitting during interphase (Fig. S1 D; Bahe et al., 2005), caused most HeLa cells to use the prophase pathway (81%), indicating that the relative timing of NEBD and centrosome separation determines which pathway is used to establish a bipolar spindle (Fig. 1 C).

We next asked whether the bipolar spindle assembly kinetics differed between the two pathways and how they were influenced by Mcm21R depletion. In untreated or control siRNA–treated cells using the prophase pathway, bipolar spindles assembled on average in 2.8 min and 3.5 min, respectively (bipolar spindle assembly duration was defined as the time between NEBD and the establishment of two MT asters linked with interpolar MTs and positioned on opposite sides of the chromosome mass; Fig. 1 D). Bipolar spindles assembled more slowly in untreated or control siRNA–treated cells using the prometaphase pathway (6.8 min and 6.6 min, respectively; Fig. 1 D). Mcm21R depletion did not affect the ratio of cells using the prophase (50%) and prometaphase pathway (50%) or the bipolar spindle assembly kinetics in the prophase pathway (Fig. 1, C–E; and Video 2, available at http://www.jcb.org/cgi/content/full/jcb.200809055/DC1). However, it delayed centrosome separation in cells using the prometaphase pathway (12.4 min; Fig. 1, D and F; and Video 3). In contrast, other monopolar spindle-inducing treatments, such as depletion of the centrosomal kinesins Eg5 or Kif2A, blocked bipolar spindle assembly in all cells irrespective of the position of centrosomes at NEBD (Fig. S1 E; Sawin et al., 1992; Blangy et al., 1995; Ganem and Compton, 2004). This suggested that Mcm21R depletion delays bipolar spindle formation only in cells that have not yet separated their centrosomes at NEBD, in contrast to Eg5 or Kif2A depletion, which block centrosome separation at all stages. Consistent with such a hypothesis, codepletion of rootletin suppressed the occurrence of monopolar spindles in Mcm21R but not in Eg5-depleted cells (Fig. 1 G and Fig. S1 F). This suppression was genuine, as double-depleted cells had Mcm21R protein levels that were as low as single *siMcm21R*-treated cells (Fig. S1, G and H).

The centrosome separation defects suggested that Mcm21R depletion affects the interface between kinetochores and the mitotic spindle. Therefore, we investigated three key kinetochore MT functions in Mcm21R-depleted cells: poleward MT flux, MT nucleation at kinetochores, and stabilization of k-fibers. To monitor the rate of poleward MT flux, we generated fluorescent marks on MTs in hTERT-RPE1 cells expressing photoactivatable (PA)-GFP–α-tubulin and recorded their movement. In control cells, the activated marks moved toward the poles at 0.8 ± 0.3 μm/min, whereas in cells lacking either the MT depolymerases mitotic centromere-associated kinesin (MCAK) and Kif2A (Fig. 2, A and B; and Videos 4 and 5, available at http://www.jcb.org/cgi/content/full/jcb.200809055/DC1) or the MT-associated proteins CLASP1 and CLASP2 (Maiato, H., personal communication), the rate of MT flux was reduced as previously described (Ganem et al., 2005; Maiato et al., 2005). Mcm21R depletion was efficient in hTERT-RPE1 cells, resulting in monopolar spindles (Fig. S1, B and C), but did not decrease flux rate (1.2 ± 0.4 μm/min; Fig. 2, A and B; and Video 6). To test for MT nucleation at kinetochores, we used a nocodazole washout assay and stained fixed cells for tubulin and centrosomes to visualize centrosomal and noncentrosomal asters (Tulu et al., 2006). Both control and Mcm21R-depleted cells contained two centrosomal asters and a mean of 5.1 and 4.3 kinetochore-associated MT asters, respectively (Fig. S1, I and J), indicating that Mcm21R depletion does not affect MT nucleation at kinetochores. To measure k-fiber stability, we cold treated cells for 10 min to depolymerize all non k-fiber MTs (Salmon and Segall, 1980) and quantified k-fiber intensity in the vicinity of kinetochores (for methodology, see Fig. S2).

Published February 9, 2009

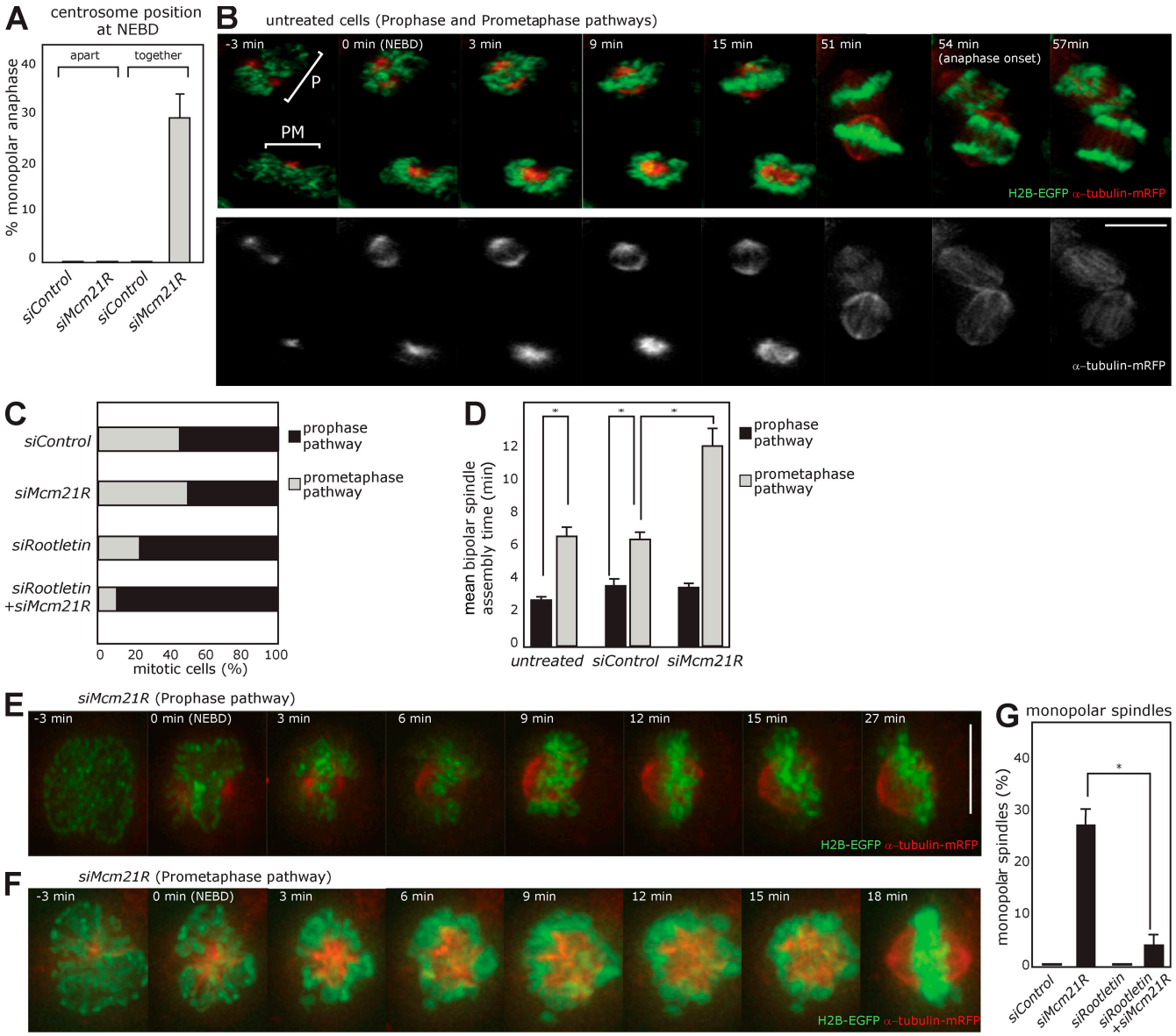

Figure 1. **Mcm21R is required for efficient bipolar spindle formation in the prometaphase pathway.** (A) Percentage of cells undergoing monopolar anaphase when centrosomes are either together or apart at the time of NEBD. (B) Successive frames every 3 min from a live cell video of HeLa cells expressing H2B-EGFP/α-tubulin–mRFP (to mark chromosomes and MTs). Images for α-tubulin–mRFP and the composite images for H2B-EGFP (green) and α-tubulin–mRFP (red) of two adjacent cells are shown. The top cell follows the prophase (P) pathway, and the bottom cell follows the prometaphase (PM) pathway. (C) Percentage of mitotic HeLa cells using either the prophase or prometaphase pathways in *siControl* ($n = 73$), *siMcm21R* ($n = 73$), *siRootletin* ($n = 31$), or *siMcm21R* + *siRootletin* ($n = 42$)–treated cells. (D) Mean bipolar spindle assembly time in the prophase or prometaphase pathway in untreated ($n = 69$) or treated with *siControl* ($n = 73$) or *siMcm21R* ($n = 73$) RNAs. (E and F) Successive frames every 3 min from a live cell video of *siMcm21R* RNA–treated cells in the prophase (E) or prometaphase (F) pathways. (G) Percentage of monopolar spindles in fixed cells after treatment with *siControl* ($n = 90$), *siMcm21R* ($n = 90$), *siRootletin* ($n = 90$), or *siMcm21R* + *siRootletin* RNAs ($n = 90$). Asterisks represent statistically significant differences ($P < 0.01$ by Mann-Whitney test). Error bars represent SEM. Bars, 10 μm.

We validated our assay by showing that kinetochores lacking Nuf2R, a subunit of the NDC80 complex required for stable kinetochore–MT attachment (DeLuca et al., 2005), also lacked stable k-fibers (78 ± 5% of kinetochores having no signal compared with 4 ± 4% in control depletion; Fig. 2, C and F). In contrast, Mcm21R depletion diminished but did not abolish the number of stable k-fibers in bipolar spindles when compared with control depletion (49 ± 6% kinetochores with a weak signal vs. 31 ± 9%, respectively; Fig. 2, C and F) and in monopolar spindles when compared with Eg5-depleted cells (Fig. 2 D). We conclude that Mcm21R depletion reduces the number of stable k-fibers, suggesting that this defect is the mechanistic cause for the centrosome separation defects.

To test our hypothesis, we investigated whether we could restabilize k-fibers and suppress the centrosome separation defects by depleting the kinetochore-bound MT depolymerase MCAK in Mcm21R-depleted cells. MCAK depletion increased k-fiber stability in wild-type cells and restabilized k-fibers in Mcm21R-depleted cells (Fig. 2, E and F). This result was genuine, as both Mcm21R and MCAK protein levels were similarly

Published February 9, 2009

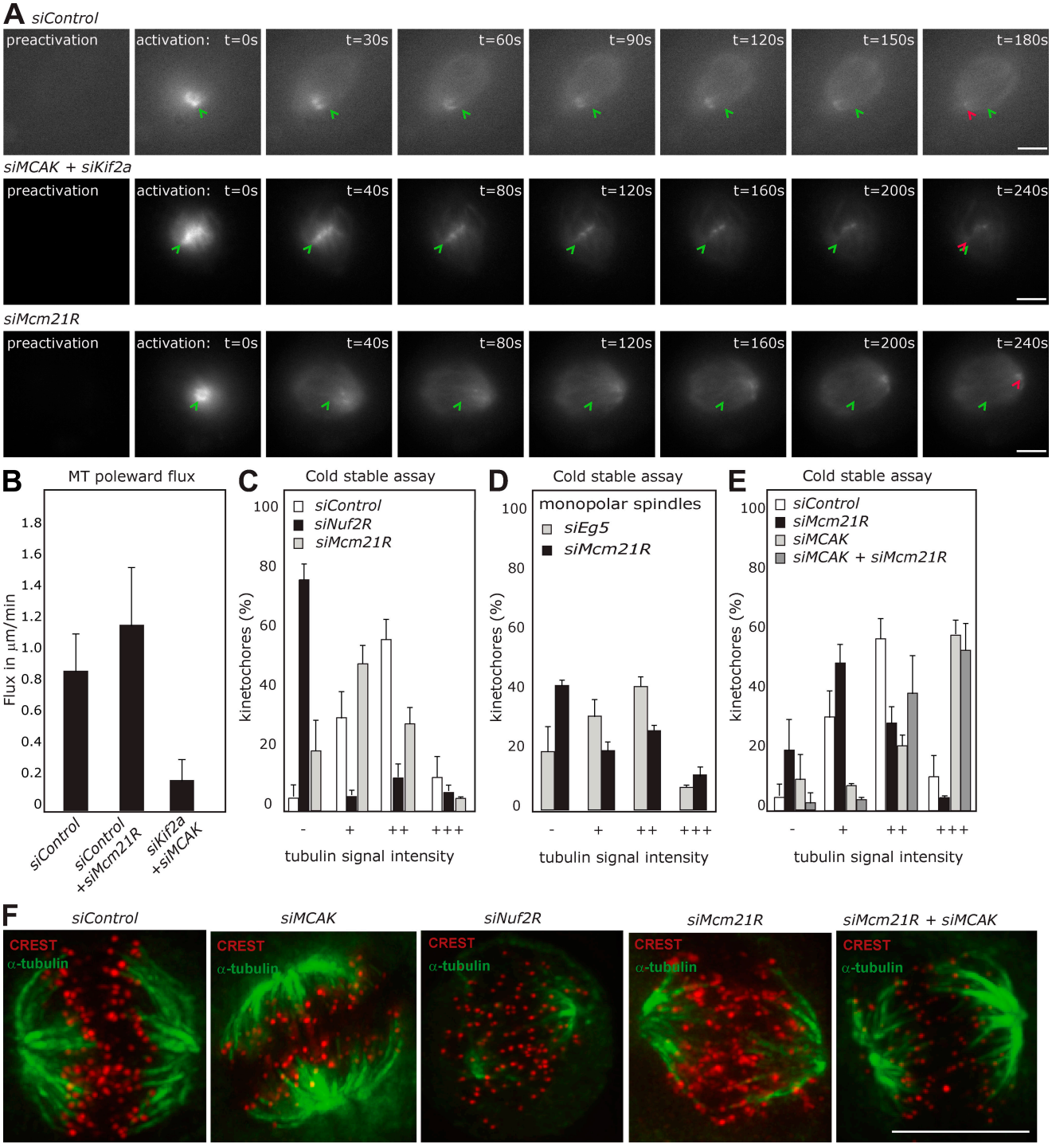

Figure 2. **Depletion of Mcm21R reduces the number of stable k-fibers.** (A) Successive frames every 30 or 40 s after photoactivation of stable PA-GFP–α-tubulin/hTERT-RPE1 cells treated either with *siControl*, *siMcm21R*, or *siMCAK* + *siKif2A* RNAs. Green arrowheads mark the initial position of a photoactivated mark, and red arrowheads show the final position of the mark. (B) Quantification of poleward MT flux rate in cells treated with *siControl* ($n = 9$), *siMcm21R* ($n = 9$), or *siMCAK* + *siKif2A* ($n = 5$) RNAs. (C–E) Quantification of stable k-fibers in cold-treated cells (for methodology, see Fig. S2, available at http://www.jcb.org/cgi/content/full/jcb.200809055/DC1). Bar graphs indicate the percentage of kinetochores lacking attached MTs (−), having a weak attachment (+), a medium attachment (++), or a strong attachment (+++) in *siControl* ($n = 354$)-, *siNuf2R* ($n = 204$)-, and *siMcm21R* ($n = 273$)-treated cells with bipolar spindles (C), in *siMcm21R* ($n = 215$)- and *siEg5* ($n = 212$)-treated cells with monopolar spindles (D), and in *siControl* ($n = 354$)-, *siMcm21R* ($n = 273$)-, *siMCAK* ($n = 238$)-, and *siMcm21R* + *siMCAK* ($n = 219$)–treated cells with bipolar spindles (E). (F) Representative images from C and E of cold-treated cells stained with α-tubulin antibodies (MTs; green) and CREST antisera (kinetochores; red). Error bars represent SEM. Bars, 10 µm.

low in the double versus single siRNA transfections (Fig. S1, K–M). MCAK depletion also rescued bipolar spindle formation timing of Mcm21R-depleted cells in prometaphase while not affecting centrosome separation in wild-type cells (Fig. 3 A), indicating that k-fiber stability determines the kinetics of centrosome separation during prssometaphase.

Published February 9, 2009

Because k-fiber stabilization is a basic function of kinetochores, we next tested whether kinetochores in general facilitate centrosome separation during prometaphase. We either abrogated k-fibers by depleting Nuf2R or weakened k-fiber stability by depleting the kinesin centromere protein E (CENP-E; Fig. S1 N; Putkey et al., 2002). Neither of these depletions affected spindle formation in the prophase pathway (not depicted); however, both treatments delayed centrosome separation during prometaphase (3.9 [*siNuf2R*] and 4.8 min [*siCENP-E*] slower than control cells; Fig. 3 B). Therefore, we conclude that kinetochores in general promote centrosome separation in cells that have not yet separated their centrosomes at NEBD.

Why would k-fiber stability facilitate centrosome separation? Previous studies demonstrated that kinetochores can produce a pushing force through poleward MT flux by incorporating tubulin subunits at the MT plus ends (Waters et al., 1996; Maiato et al., 2005). In *Drosophila melanogaster*, this force is essential for bipolar spindle maintenance but not for spindle assembly (Maiato et al., 2002). We propose that in human cells, kinetochores push the centrosomes apart during prometaphase using poleward MT flux and hypothesize that reducing the number of stable k-fibers delays centrosome separation by decreasing the net force generated by MT flux. Such a model predicts that Mcm21R depletion should diminish the number of growing MTs within the spindle. Consistently, Mcm21R depletion severely reduced the abundance of spindle-associated EB1, which is a marker for growing MTs (Fig. 3 C; Tirnauer et al., 2002). A second prediction is that diminished MT flux should delay bipolar spindle formation. A previous fixed-cell study showed that loss of flux in human cells induced by depletion of Kif2A and MCAK allows bipolar spindle formation (Ganem et al., 2005). However, our live cell assay demonstrates that depletion of MCAK and Kif2A delays bipolar spindle formation in the prometaphase pathway (5.6 min slower; Fig. 3 B). Consistent with a role of MT flux in centrosome separation, we also observed a severe delay in cells depleted of CLASP1/2 (12.2 min slower; Fig. 3 B and Video 7, available at http://www.jcb.org/cgi/content/full/jcb.200809055/DC1; for an immunoblot showing depletion of CLASP1/2 by siRNA treatment, see Fig. S1 O). In contrast to Kif2A/MCAK-depleted cells, CLASP1/2-depleted cells nearly always used the prometaphase pathway and often formed multipolar spindles (Fig. S1 P and not depicted), suggesting that CLASP1/2 also regulate other aspects of spindle assembly.

An important question is why loss of the kinetochore-driven pushing force delays centrosome separation but does not block it. A likely reason is the redundancy of the pathways that promote bipolar spindle formation and centrosome separation in particular cortical forces (Walczak and Heald, 2008). Because aurora A is an important regulator of these forces, we tested how k-fiber destabilization affected centrosome separation when aurora A (but not aurora B) is depleted (Fig. S3 A, available at http://www.jcb.org/cgi/content/full/jcb.200809055/DC1; Barr and Gergely, 2007). In Mcm21R-depleted cells, codepletion of aurora A blocked centrosome separation during the first 15 min after NEBD (Mcm21R-depleted cells then entered anaphase as a result of a deficient spindle checkpoint)

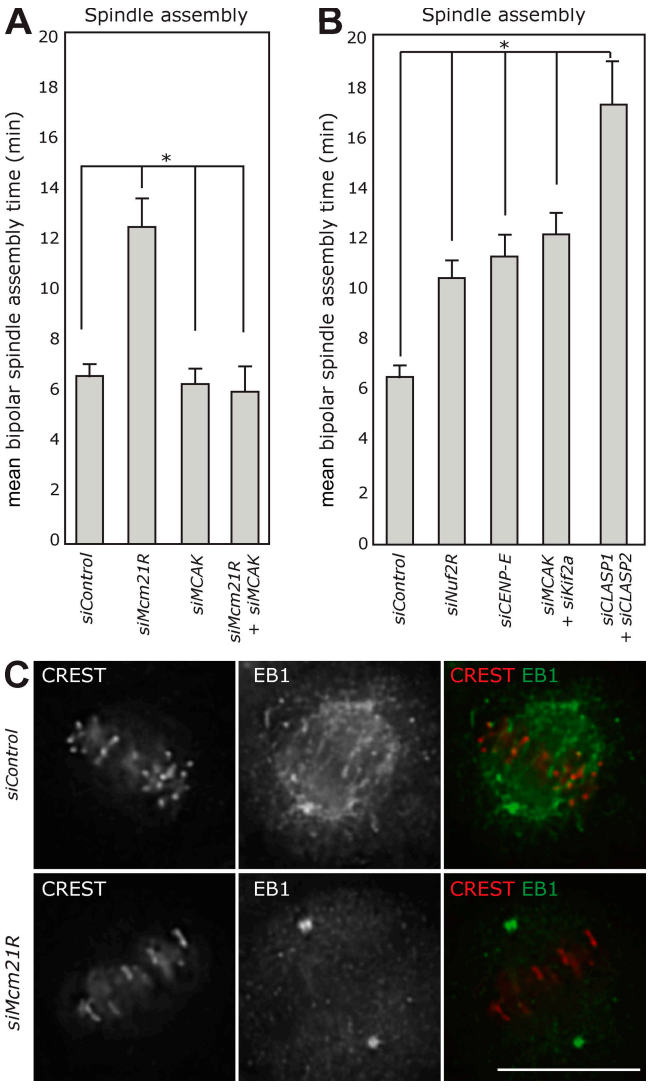

Figure 3. **Kinetochores and poleward MT flux are required for timely centrosome separation.** (A and B) Mean bipolar spindle formation time in the prometaphase pathway in *siControl* (n = 38)-, *siMcm21R* (n = 36)-, *siMCAK* (n = 23)-, or *siMcm21R* + *siMCAK* (n = 31)–treated cells (A) or in *siControl* (n = 38)-, *siNuf2R* (n = 40)-, *siCENP-E* (n = 28)–, *siMCAK* + *siKif2A* (n = 38)–, or *siCLASP1* + *siCLASP2* (n = 28)–treated cells (B). (C) Representative images of *siControl*- or *siMcm21R* RNA–treated cells stained with CREST antisera (to mark kinetochores) and EB1 antisera (to mark growing MT plus ends). Asterisks indicate statistically significant differences ($P < 0.01$ by Mann-Whitney test). Error bars represent SEM. Bar, 10 μm.

in the prometaphase pathway but not in the prophase pathway while producing only a minor delay in control-depleted cells (Fig. 4 A and Fig. S3 B). The depletion of aurora A and/or Mcm21R was confirmed by quantitative immunofluorescence (Fig. S3, C–E). This synergistic effect was specific for aurora A, as the aurora B inhibitor ZM1 did not block centrosome separation in Mcm21R-depleted cells (Fig. 4 A; Ditchfield et al., 2003). Aurora A depletion also blocked centrosome separation in Nuf2R-, CENP-E–, and Kif2A/MCAK-depleted cells using the prometaphase pathway, indicating that this represents a general response (Fig. 4, A and B; and Videos 8–10; all double siRNA depletions were confirmed by quantitative immunofluorescence or immunoblotting; Fig. S3, F–J). Therefore, we conclude that

Published February 9, 2009

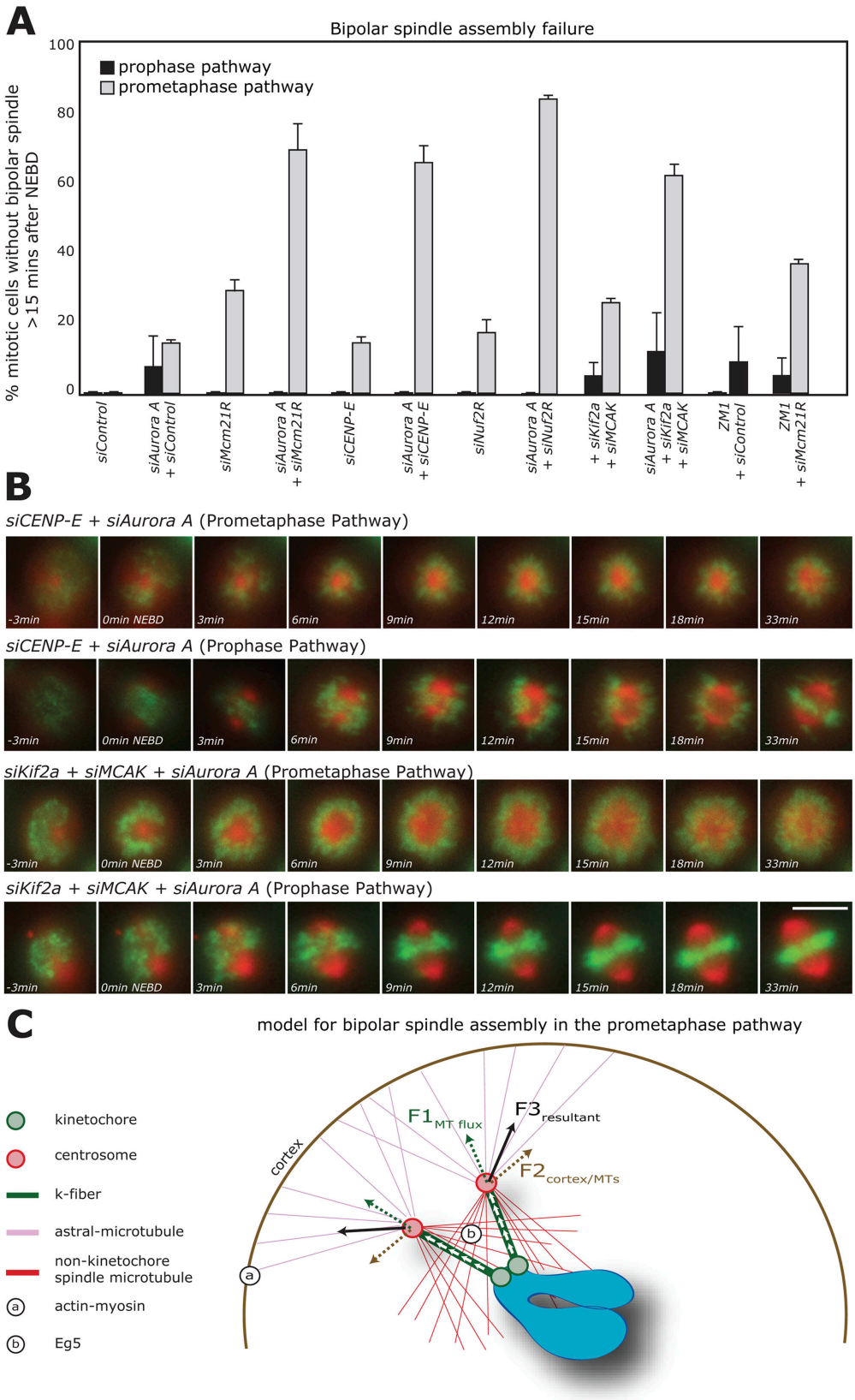

Figure 4. **Kinetochore and aurora A activities cooperate to drive centrosome separation.** (A) Percentage of cells that fail to establish a bipolar spindle within 15 min after NEBD using either the prophase or prometaphase pathway. Cells were treated with *siControl* ($n = 73$), *siMcm21R* ($n = 73$), *siaurora A + siControl* ($n = 40$), *siaurora A + siMcm21R* ($n = 38$), *siCENP-E* ($n = 42$), *siaurora A + siCENP-E* ($n = 32$), *siNuf2R* ($n = 99$), *siaurora A + siNuf2R* ($n = 20$), *siMCAK + siKif2A* ($n = 79$), *siaurora A + siKif2A + siMCAK* ($n = 52$), *siControl + ZM1* ($n = 33$), or *siMcm21R + ZM1* ($n = 46$). (B) Composite images of HeLa H2B-EGFP (green) and α-tubulin–mRFP (red) cells treated with *siaurora A + siCENP-E* or *siaurora A + siKif2A + siMCAK* in the prophase or prometaphase pathways. (C) Proposed model for the function of kinetochores in bipolar spindle formation during prometaphase. Just after NEBD, centrosomes

Published February 9, 2009

kinetochore-based poleward MT flux is rate limiting for centrosome separation in cells lacking aurora A, indicating that centrosomal- and kinetochore-based processes drive prometaphase centrosome separation in a redundant manner.

Previous studies found that bipolar spindle formation does not require kinetochores (Heald et al., 1996; Bucciarelli et al., 2003; Ganem and Compton, 2004). Our data show that kinetochores promote centrosome separation within the prometaphase pathway, which acts as a backup when centrosomes fail to separate before NEBD. This backup pathway provides redundancy and robustness to spindle bipolarity and segregates chromosomes as efficiently as the prophase pathway when measured by live cell imaging (Fig. S3 K).

Interestingly, the prometaphase pathway also requires myosin II, which localizes to the cell cortex (Rosenblatt et al., 2004). We propose that a kinetochore-based pushing force (F1) combines with cortical forces (mediated by actin and myosin) and extensile MT sliding (mediated by Eg5 [F2]) to generate a force with sufficient magnitude and correct directionality (F3) to accelerate centrosome separation in prometaphase (Fig. 4 C). Loss of k-fibers and thus MT flux slows centrosome separation by reducing the overall force that separates centrosomes. Our model predicts that as centrosomes separate from each other, the kinetochore-based pushing force will make a greater contribution to the overall forces. Consistent with this idea, kinetochore forces are not sufficient to drive bipolar spindle formation when centrosomes have collapsed together after inhibition of Eg5 (i.e., massive reduction in F2; Sawin et al., 1992; Blangy et al., 1995). However, kinetochores are critical for bipolar spindle assembly when aurora A kinase, which controls F2 through astral MTs stabilization and regulation of Eg5 (Barr and Gergely, 2007), is depleted. The kinetochore-based force provides robustness to centrosome separation, explaining the results of previous studies, which found that in endpoint assays, bipolar spindle assembly does not require kinetochores (Heald et al., 1996; Bucciarelli et al., 2003; Ganem and Compton, 2004). We speculate that the role of kinetochores in centrosome separation becomes only visible in fixed cells depleted of Mcm21R (as opposed to MCAK/Kif2A, Nuf2R, CENP-E, or CLASP1/2) because it is the only siRNA treatment that leads to a rapid entry into anaphase (McAinsh et al., 2006). In contrast, other treatments either have no effect or delay mitotic timing (Meraldi et al., 2004; Ganem et al., 2005; and unpublished data), thus giving most cells sufficient time to fully separate their centrosomes.

Kinetochore- and centrosome-based force generation are not insulated from each other but are functionally coupled; e.g., depletion of centrosome-bound Kif2A causes kinetochores to depolymerize MT plus ends, thus pulling the centrosomes together and leading to spindle collapse (Ganem and Compton, 2004), whereas our data show that in cells with unperturbed centrosomes, kinetochores push the centrosomes apart. A similar relationship exists with regard to kinetochore geometry. In cells lacking centrosomes, defective kinetochore geometry (i.e., both kinetochores facing the same side of chromosomes while attached to k-fibers) blocks spindle bipolarity (Loncarek et al., 2007). However, in our experiment with unperturbed centrosomes, the generation of the same geometry defect (as induced by aurora B inhibition) has no effect on centrosome separation. Thus, the impact of kinetochores on bipolar spindle assembly depends on the status of centrosomes. Because somatic animal cells contain centrosomes, a crucial future aim will be to understand the detailed mechanisms by which kinetochore- and centrosome-based activities are coordinated to drive centrosome separation.

Materials and methods

HeLa and HeLa H2B-EGFP/α-tubulin–mRFP were grown as described previously (McAinsh et al., 2006). hTERT-RPE1 and hTERT-RPE1 PA-GFP–α-tubulin cell lines (generated by transfection of hTERT-RPE1 cells with a PA-GFP–α-tubulin vector [pMC169] and stable clones selected with 400 μg/ml G418) were grown in 50:50 Ham's F12/DME + 10% FCS. Live cell imaging experiments were performed in chambers (Lab-Tek II; Thermo Fisher Scientific) with Leibovitz L-15 medium (Invitrogen) + 10% FCS at 37°C.

siRNA oligonucleotides (*siControl*; Allstar; QIAGEN), Nuf2R (Meraldi et al., 2004), Mcm21R (5′-ATATGAGTCTGGTCTCCTA-3′), aurora A (Marumoto et al., 2003), Kif2A (Ganem and Compton, 2004), Eg5 (5′-GGAAUUGAUUAAUGUACUC-3′; provided by D. Gerlich, Swiss Federal Institute of Technology, Zurich, Switzerland), rootletin (Bahe et al., 2005), MCAK (Cassimeris and Morabito, 2004), CLASP1 (5′-GCCAUUAUGCCAACUAUCU-3′), CLASP2 (5′-GACAUACAUGGGUCUUAGA-3′), and CENP-E (Meraldi and Sorger, 2005) were transfected as described previously (Elbashir et al., 2001). ZM1 was applied as described previously (Ditchfield et al., 2003).

Immunoblotting, immunofluorescence quantification, and live cell imaging were performed as described previously (McClelland et al., 2007). Fluorescence images were acquired with a 100× oil NA 1.4 objective (immunofluorescence) or with a 40× oil NA 1.3 objective (live cell imaging) on a microscope (Deltavision RT; Applied Precision, LLC) equipped with a camera (CoolSNAP HQ; Roper Scientific). Image stacks were deconvolved and quantified with SoftWorx (Applied Precision, LLC) and mounted in figures using Photoshop and Illustrator (Adobe). The following primary antibodies were used for immunofluorescence: CREST (1:500; Antibodies Inc.), mouse anti–α-tubulin (1:10,000; Sigma-Aldrich), rabbit anti–γ-tubulin (1:1,000; Sigma-Aldrich), rabbit anti-Mcm21R (McAinsh et al., 2006), rabbit anti–aurora A (1:1,500; Novus Biologicals), rabbit anti-MCAK (1:1,000; Cytoskeleton, Inc.), mouse anti-EB1 (1:500; BD), mouse GT-335 (1: 1,000; provided by C. Janke, Macromolecular Biochemistry Research Center, Montpellier, France), and mouse anti–CENP-A (1:1,000; Abcam). For the cold-stable assay cells, we used the methodology described in Fig. S2. To determine the degree of centrosome splitting, we used SoftWorx to measure the distance between the two interphase centrosomes stained with γ-tubulin antibodies and considered them split if the distance was >2 μm.

Bipolar assembly times were obtained from live cell imaging, and distributions and means were statistically evaluated according to the Mann-Whitney test. Photoactivation experiments were performed on bipolar metaphase spindles (identified by phase-contrast microscopy) as described

are positioned on the same side of the chromatin (blue). Sister kinetochores are in close proximity, face the centrosomes, and are connected to centrosomes via k-fibers, thereby establishing a triangular geometry. A pushing force from kinetochores (F1) based on plus end MT polymerization (poleward MT flux; white arrows) drives centrosomes apart from each other. F1 is combined with additional forces (F2), which include astral MT–cortex interactions (mediated by actin-myosin) and extensile MT sliding (mediated by Eg5), which are two processes under the control of the aurora A kinase activity. The resultant force (F3) has an altered magnitude and directionality, which allows more efficient centrosome separation. Note that the centrosome–kinetochore geometry, and therefore the magnitude and direction of forces, will evolve dynamically as the spindle forms into a structure under force balance. Error bars represent SEM. Bar, 10 μm.

previously (Ganem et al., 2005) using a 100-ns pulse from a 406-nm laser on a microscope (Deltavision RT) equipped with a quantifiable laser module (Applied Precision, LLC). Fluorescence images were captured every 10 s using a 100× oil NA 1.4 objective and FITC filter set (Applied Precision, LLC).

Online supplemental material

Fig. S1 shows the frequency of the prophase and prometaphase pathways and the phenotype of Mcm21R depletion in hTERT-RPE1 cells. We also show experiments confirming the single and double depletions of Mcm21R, rootletin, MCAK, CLASP1, CLASP2, and CENP-E after siRNA treatment used in this study. Finally, we show how depletion of Mcm21R does not affect MT nucleation at kinetochores and how Kif2A/MCAK or CLASP1/2 double depletions affect the frequency at which HeLa cells use either the prometaphase or prophase pathways. Fig. S2 provides a detailed description of the methodology used to determine the number of cold-stable k-fibers. In Fig. S3, we confirm the efficiency of the single, double, and triple depletions of Mcm21R, aurora A, aurora B, Nuf2R, CENP-E, MCAK, and Kif2A that were used in this study. We also show how depletion of aurora A affects the timing of bipolar spindle formation in the prophase and prometaphase pathways. Finally, we show that the number of chromosome segregation errors is similar in cells using prophase or prometaphase pathways. Video 1 shows H2B-EGFP/α-tubulin–mRFP cells, with one following the prometaphase pathway, and one following the prophase pathway. Videos 2 and 3 show an Mcm21R-depleted H2B-EGFP/α-tubulin–mRFP cell following the prophase pathway (Video 2) or prometaphase pathway (Video 3). Videos 4–6 show MT flux after photoactivation of PA-GFP–α-tubulin in a control (Video 4), Mcm21R (Video 6), and Kif2A/MCAK (Video 5)-depleted cell. Videos 7 and 8 show H2B-EGFP/α-tubulin–mRFP cells treated with *siCLASP1/siCLASP2* (Video 7) or with *siMCAK/siKif2A/siaurora A* (Video 8) in the prometaphase pathway. Videos 9 and 10 show *siaurora A/siCENP-E*–treated H2B-EGFP/α-tubulin–mRFP cells in the prometaphase (Video 9) or prophase (Video 10) pathways. Online supplemental material is available at http://www.jcb.org/cgi/content/full/jcb.200809055/DC1.

We thank the Light Microscopy Centre of the ETH Zurich for technical support, Helder Maiato (Instituto de Biologia Molecular e Celular, Porto, Portugal) for CLASP1/2 siRNA sequences and for sharing unpublished results, Daniel Gerlich for Eg5 siRNA, Niels Galjart (Erasmus Medical Center, Rotterdam, Netherlands) for CLASP1/2 antibodies, Carsten Janke for GT335 antibodies, and Andreas Essig, Joëlle Sasse, and Sabina Reggi for characterizing rootletin RNAi. We are grateful to Yves Barral, Rob Cross, Monica Gotta, and Ulrike Kutay for critical reading of the manuscript and members of the McAinsh and Meraldi laboratories for discussions.

Work in the McAinsh laboratory was supported by Marie Curie Cancer Care (grants to A.D. McAinsh, A.J. Garrod, and J.R. Winter). A. Toso and A.C. Amaro are members of the Life Science Zurich Graduate School in molecular life science. P. Meraldi is the recipient of a Swiss National Science Foundation–Förderungprofessur award and a European Young Investigator award and is supported by a Swiss National Science Foundation grant.

Submitted: 8 September 2008
Accepted: 8 January 2009

References

Bahe, S., Y.D. Stierhof, C.J. Wilkinson, F. Leiss, and E.A. Nigg. 2005. Rootletin forms centriole-associated filaments and functions in centrosome cohesion. *J. Cell Biol.* 171:27–33.

Barr, A.R., and F. Gergely. 2007. Aurora-A: the maker and breaker of spindle poles. *J. Cell Sci.* 120:2987–2996.

Barr, F.A., H.H. Sillje, and E.A. Nigg. 2004. Polo-like kinases and the orchestration of cell division. *Nat. Rev. Mol. Cell Biol.* 5:429–440.

Blangy, A., H.A. Lane, P. d'Herin, M. Harper, M. Kress, and E.A. Nigg. 1995. Phosphorylation by p34cdc2 regulates spindle association of human Eg5, a kinesin-related motor essential for bipolar spindle formation in vivo. *Cell.* 83:1159–1169.

Bucciarelli, E., M.G. Giansanti, S. Bonaccorsi, and M. Gatti. 2003. Spindle assembly and cytokinesis in the absence of chromosomes during *Drosophila* male meiosis. *J. Cell Biol.* 160:993–999.

Cassimeris, L., and J. Morabito. 2004. TOGp, the human homolog of XMAP215/Dis1, is required for centrosome integrity, spindle pole organization, and bipolar spindle assembly. *Mol. Biol. Cell.* 15:1580–1590.

DeLuca, J.G., Y. Dong, P. Hergert, J. Strauss, J.M. Hickey, E.D. Salmon, and B.F. McEwen. 2005. Hec1 and nuf2 are core components of the kinetochore outer plate essential for organizing microtubule attachment sites. *Mol. Biol. Cell.* 16:519–531.

Ditchfield, C., V.L. Johnson, A. Tighe, R. Ellston, C. Haworth, T. Johnson, A. Mortlock, N. Keen, and S.S. Taylor. 2003. Aurora B couples chromosome alignment with anaphase by targeting BubR1, Mad2, and Cenp-E to kinetochores. *J. Cell Biol.* 161:267–280.

Elbashir, S.M., J. Harborth, W. Lendeckel, A. Yalcin, K. Weber, and T. Tuschl. 2001. Duplexes of 21-nucleotide RNAs mediate RNA interference in cultured mammalian cells. *Nature.* 411:494–498.

Foltz, D.R., L.E. Jansen, B.E. Black, A.O. Bailey, J.R. Yates III, and D.W. Cleveland. 2006. The human CENP-A centromeric nucleosome-associated complex. *Nat. Cell Biol.* 8:458–469.

Ganem, N.J., and D.A. Compton. 2004. The KinI kinesin Kif2a is required for bipolar spindle assembly through a functional relationship with MCAK. *J. Cell Biol.* 166:473–478.

Ganem, N.J., K. Upton, and D.A. Compton. 2005. Efficient mitosis in human cells lacking poleward microtubule flux. *Curr. Biol.* 15:1827–1832.

Heald, R., R. Tournebize, T. Blank, R. Sandaltzopoulos, P. Becker, A. Hyman, and E. Karsenti. 1996. Self-organization of microtubules into bipolar spindles around artificial chromosomes in *Xenopus* egg extracts. *Nature.* 382:420–425.

Heald, R., R. Tournebize, A. Habermann, E. Karsenti, and A. Hyman. 1997. Spindle assembly in *Xenopus* egg extracts: respective roles of centrosomes and microtubule self-organization. *J. Cell Biol.* 138:615–628.

Loncarek, J., O. Kisurina-Evgenieva, T. Vinogradova, P. Hergert, S. La Terra, T.M. Kapoor, and A. Khodjakov. 2007. The centromere geometry essential for keeping mitosis error free is controlled by spindle forces. *Nature.* 450:745–749.

Maiato, H., P. Sampaio, C.L. Lemos, J. Findlay, M. Carmena, W.C. Earnshaw, and C.E. Sunkel. 2002. MAST/Orbit has a role in microtubule–kinetochore attachment and is essential for chromosome alignment and maintenance of spindle bipolarity. *J. Cell Biol.* 157:749–760.

Maiato, H., A. Khodjakov, and C.L. Rieder. 2005. *Drosophila* CLASP is required for the incorporation of microtubule subunits into fluxing kinetochore fibres. *Nat. Cell Biol.* 7:42–47.

Marumoto, T., S. Honda, T. Hara, M. Nitta, T. Hirota, E. Kohmura, and H. Saya. 2003. Aurora-A kinase maintains the fidelity of early and late mitotic events in HeLa cells. *J. Biol. Chem.* 278:51786–51795.

McAinsh, A.D., P. Meraldi, V.M. Draviam, A. Toso, and P.K. Sorger. 2006. The human kinetochore proteins Nnf1R and Mcm21R are required for accurate chromosome segregation. *EMBO J.* 25:4033–4049.

McClelland, S.E., S. Borusu, A.C. Amaro, J.R. Winter, M. Belwal, A.D. McAinsh, and P. Meraldi. 2007. The CENP-A NAC/CAD kinetochore complex controls chromosome congression and spindle bipolarity. *EMBO J.* 26:5033–5047.

Meraldi, P., and P.K. Sorger. 2005. A dual role for Bub1 in the spindle checkpoint and chromosome congression. *EMBO J.* 24:1621–1633.

Meraldi, P., V.M. Draviam, and P.K. Sorger. 2004. Timing and checkpoints in the regulation of mitotic progression. *Dev. Cell.* 7:45–60.

Putkey, F.R., T. Cramer, M.K. Morphew, A.D. Silk, R.S. Johnson, J.R. McIntosh, and D.W. Cleveland. 2002. Unstable kinetochore-microtubule capture and chromosomal instability following deletion of CENP-E. *Dev. Cell.* 3:351–365.

Rosenblatt, J. 2005. Spindle assembly: asters part their separate ways. *Nat. Cell Biol.* 7:219–222.

Rosenblatt, J., L.P. Cramer, B. Baum, and K.M. McGee. 2004. Myosin II-dependent cortical movement is required for centrosome separation and positioning during mitotic spindle assembly. *Cell.* 117:361–372.

Salmon, E.D., and R.R. Segall. 1980. Calcium-labile mitotic spindles isolated from sea urchin eggs (*Lytechinus variegatus*). *J. Cell Biol.* 86:355–365.

Sawin, K.E., K. LeGuellec, M. Philippe, and T.J. Mitchison. 1992. Mitotic spindle organization by a plus-end-directed microtubule motor. *Nature.* 359:540–543.

Tirnauer, J.S., J.C. Canman, E.D. Salmon, and T.J. Mitchison. 2002. EB1 targets to kinetochores with attached, polymerizing microtubules. *Mol. Biol. Cell.* 13:4308–4316.

Tulu, U.S., C. Fagerstrom, N.P. Ferenz, and P. Wadsworth. 2006. Molecular requirements for kinetochore-associated microtubule formation in mammalian cells. *Curr. Biol.* 16:536–541.

Walczak, C.E., and R. Heald. 2008. Mechanisms of mitotic spindle assembly and function. *Int. Rev. Cytol.* 265:111–158.

Waters, J.C., T.J. Mitchison, C.L. Rieder, and E.D. Salmon. 1996. The kinetochore microtubule minus-end disassembly associated with poleward flux produces a force that can do work. *Mol. Biol. Cell.* 7:1547–1558.

Published February 9, 2009

Supplemental Material

JCB

Toso et al., http://www.jcb.org/cgi/content/full/jcb.200809055/DC1

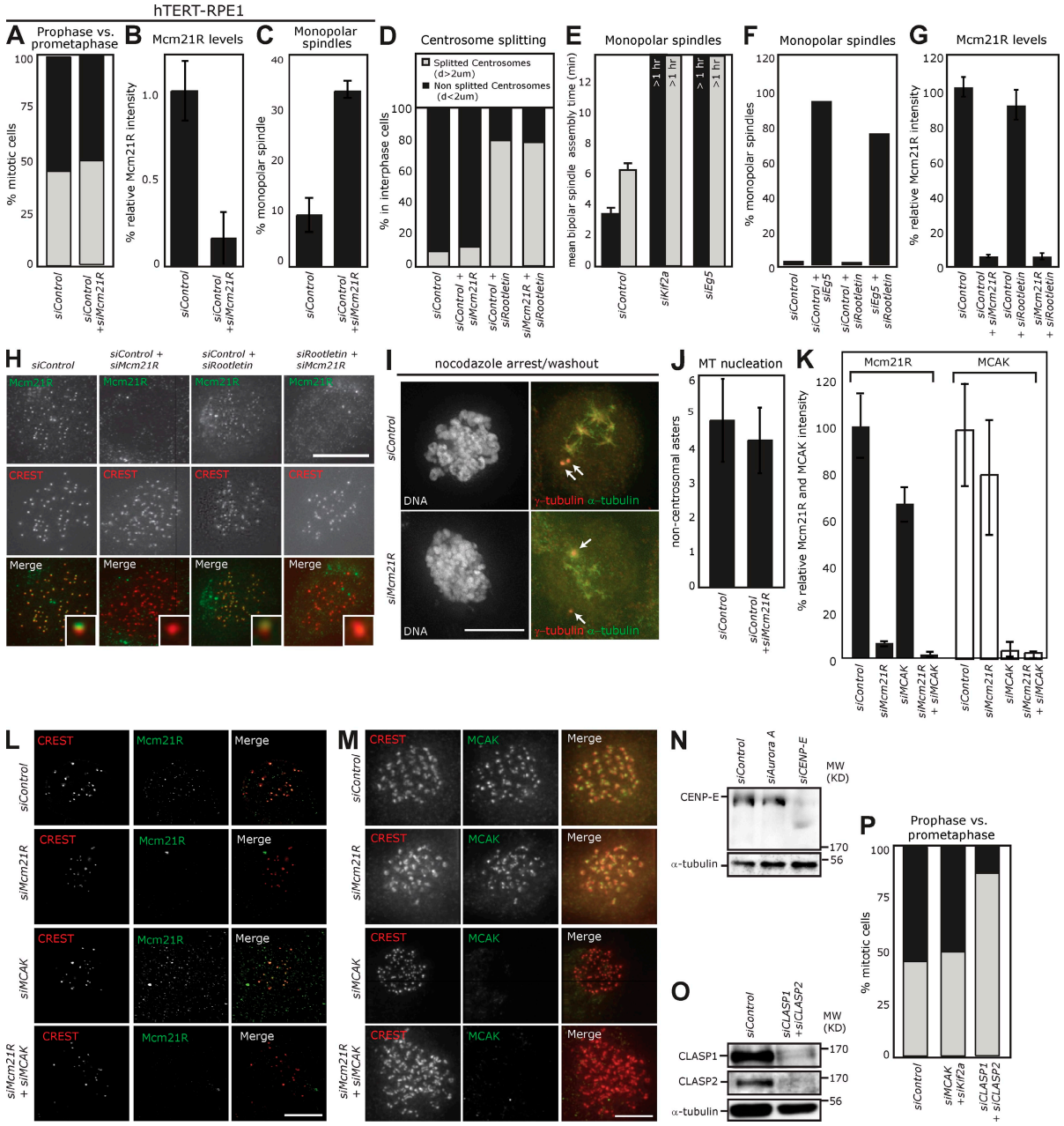

Figure S1. **Control experiments for siRNA depletions used in Figs. 1–3.** The phenotype of Mcm21R depletion in diploid hTERT-RPE1 cells and evidence that Mcm21R depletion does not affect MT nucleation at kinetochores. (A) Percentage of mitotic hTERT-RPE1 cells using either the prophase (black bars) or prometaphase pathways (gray bars) in *siControl*- or *siMcm21R*-treated cells. (B) Quantification of Mcm21R protein levels on kinetochores of *siControl*- or *siMcm21R*-treated cells as determined from deconvolved 3D reconstructions of hTERT-RPE1 cells stained with Mcm21R and CREST antisera as described previously (McClelland, S.E., S. Borusu, A.C. Amaro, J.R. Winter, M. Belwal, A.D. McAinsh, and P. Meraldi. 2007. *EMBO J.* 26:5033–5047). (C) Fraction of cells with monopolar spindles in hTERT-RPE1 cells treated with *siControl* or *siMcm21R* RNAs. (D) Functional assay for centrosome splitting in interphase to confirm depletion of rootletin by siRNA treatment. The percentage of interphase cells with split or unsplit centrosomes after treatment with siRNAs as indicated is shown. (E) Mean bipolar spindle assembly time in *siControl*-, *siKif2a*-, or *siEg5*-treated cells. (F) Percentage of monopolar spindles 12 min after NEBD after treatment with *siControl*, *siControl* + *siEg5*, *siControl* + *siRootletin*, or *siEg5* + *siRootletin* RNAs. (G) Immunofluorescence quantification of Mcm21R levels on kinetochores from deconvolved 3D reconstructions of cells stained with CREST antisera (kinetochores) and Mcm21R antibodies (McClelland et al., 2007) after treatment with *siControl*, *siMcm21R*, *siRootletin*, or *siMcm21R* + *siRootletin* RNAs. (H) Representative images are shown, and insets show higher magnification views of a single kinetochore. (I and J) Quantification of MT nucleation at kinetochores in control and Mcm21R-depleted cells. (I) Representative images of cells transfected with *siControl* or *siMcm21R* RNAs treated with 3.3 mM nocodazole for 3.5 h followed by wash and release into fresh media for 13 min before fixing and staining with DAPI (to mark DNA), α-tubulin (green), and γ-tubulin (red) antibodies. Arrows indicate centrosomal asters. (J) Quantification of noncentrosomal (kinetochore) asters from cells treated as in I. (K–M) Levels of Mcm21R and MCAK on kinetochores in cells stained with CREST antisera (kinetochores) and Mcm21R or MCAK antibodies after treatment with *siControl*, *siMcm21R*, *siMCAK*, or *siMcm21R* + *siMCAK* RNAs. Representative images are shown in L and M. (N) Depletion of CENP-E. Immunoblots of whole cell lysates from cells treated with *siControl*, *siaurora A*, or *siCENP-E* RNAs and probed with CENP-E or α-tubulin antibodies are shown. (O) Depletion of CLASP1/2. Immunoblots of whole cell lysates from cells treated with *siControl* or *siCLASP1* + *siCLASP2* RNAs and probed with CLASP1, CLASP2, or α-tubulin antibodies are shown. (P) Percentage of HeLa cells using either the prophase (black bars) or prometaphase pathways (gray bars) in *siControl*-, *siMCAK* + *siKif2a*–, or *siCLASP1* + *siCLASP2*–treated cells. MW, molecular weight. Error bars represent SEM. Bars, 10 μm.

Published February 9, 2009

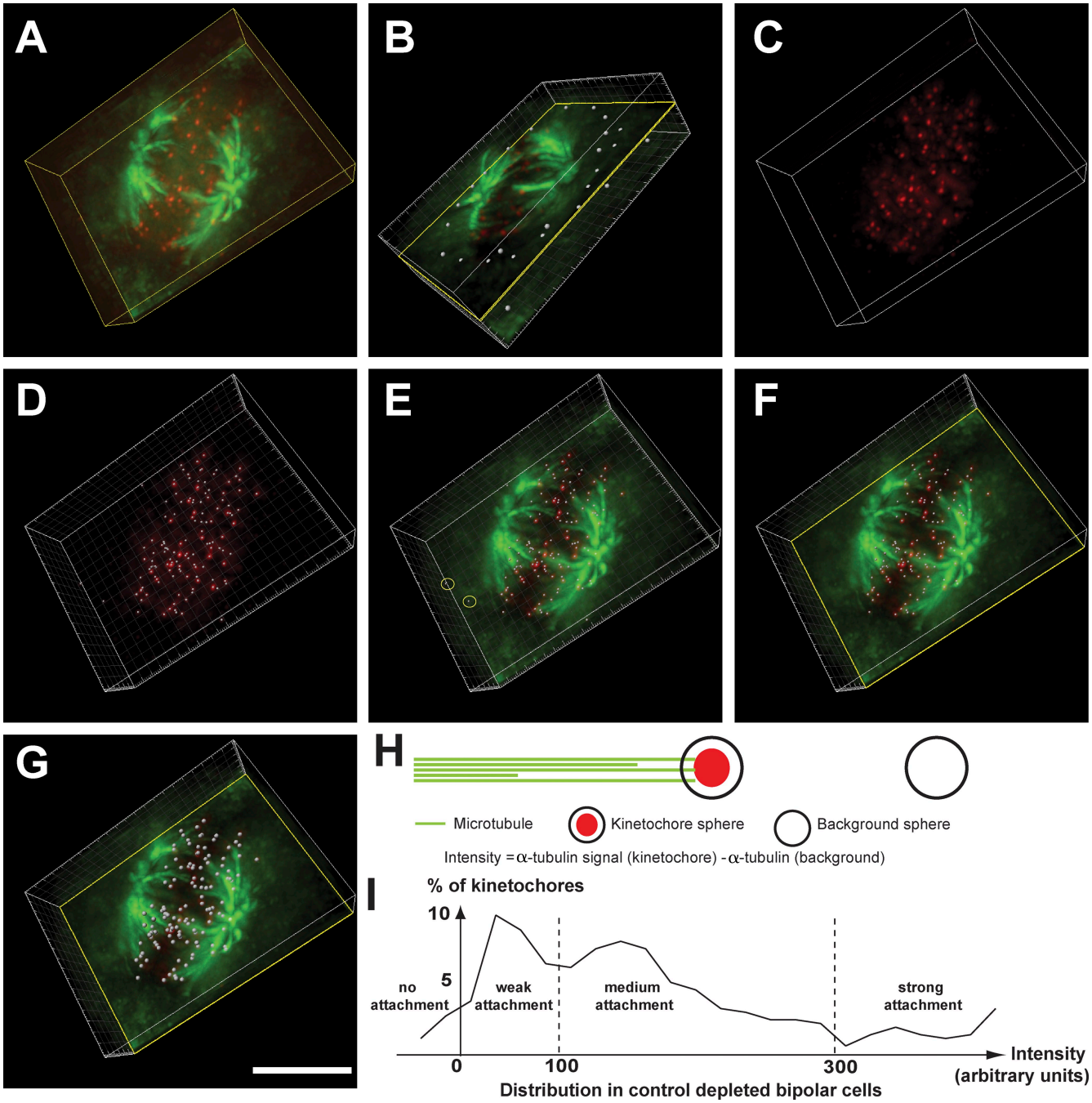

Figure S2. **Determination of numbers of cold-stable k-fibers.** For the cold-stable assay, cells were incubated in ice-cold medium 10 min before 6 min fixation with −20°C methanol. Cells were stained for immunofluorescence with mouse anti–α-tubulin and human CREST antibodies. Image stacks in 0.3-mm steps were acquired with a 100× oil NA 1.4 objective on a microscope (RT Deltavision; Applied Precision, LLC) and deconvolved with SoftWorx (Applied Precision, LLC) as described previously (McClelland et al., 2007). (A) Image stacks were transferred into IMARIS 5.7 (Bitplane). (B) The mean background of the α-tubulin channel (green) was determined by manually placing 20–30 spheres (gray) with a diameter of 0.65 µm outside the mitotic spindle. (C) The green channel was temporarily removed. (D) CREST-stained kinetochores were automatically detected using the IMARIS spot detection function (minimum diameter of 0.3 µm) with a >99% accuracy, as determined by visual inspection (white dots). (E) The green α-tubulin channel was reinserted, and the rare unspecific spots located in a large distance outside of the mitotic spindle were manually marked (yellow circles). (F) The unspecific spots were removed. (G) The diameter of every detected kinetochore sphere was expanded to 0.65 µm (gray spheres). (H) The intensity of the α-tubulin channel was measured within each 0.65-µm sphere, and the mean background determined in B was subtracted. (I) For each siRNA condition, the individual intensities of cold-stable k-fibers were determined in five cells with at least 40 kinetochores per cell, yielding a distribution of at least 200 k-fiber intensities. The distribution in control-depleted cells was typically bimodal and was subdivided into four categories. Values below background were designated as kinetochores with no attachment, values in the first peak (0–100) were categorized as weak attachments, values in the second largest peak (100–300) were categorized as medium attachments, and values above (>300) were considered as strong attachments. Bar, 10 µm.

Published February 9, 2009

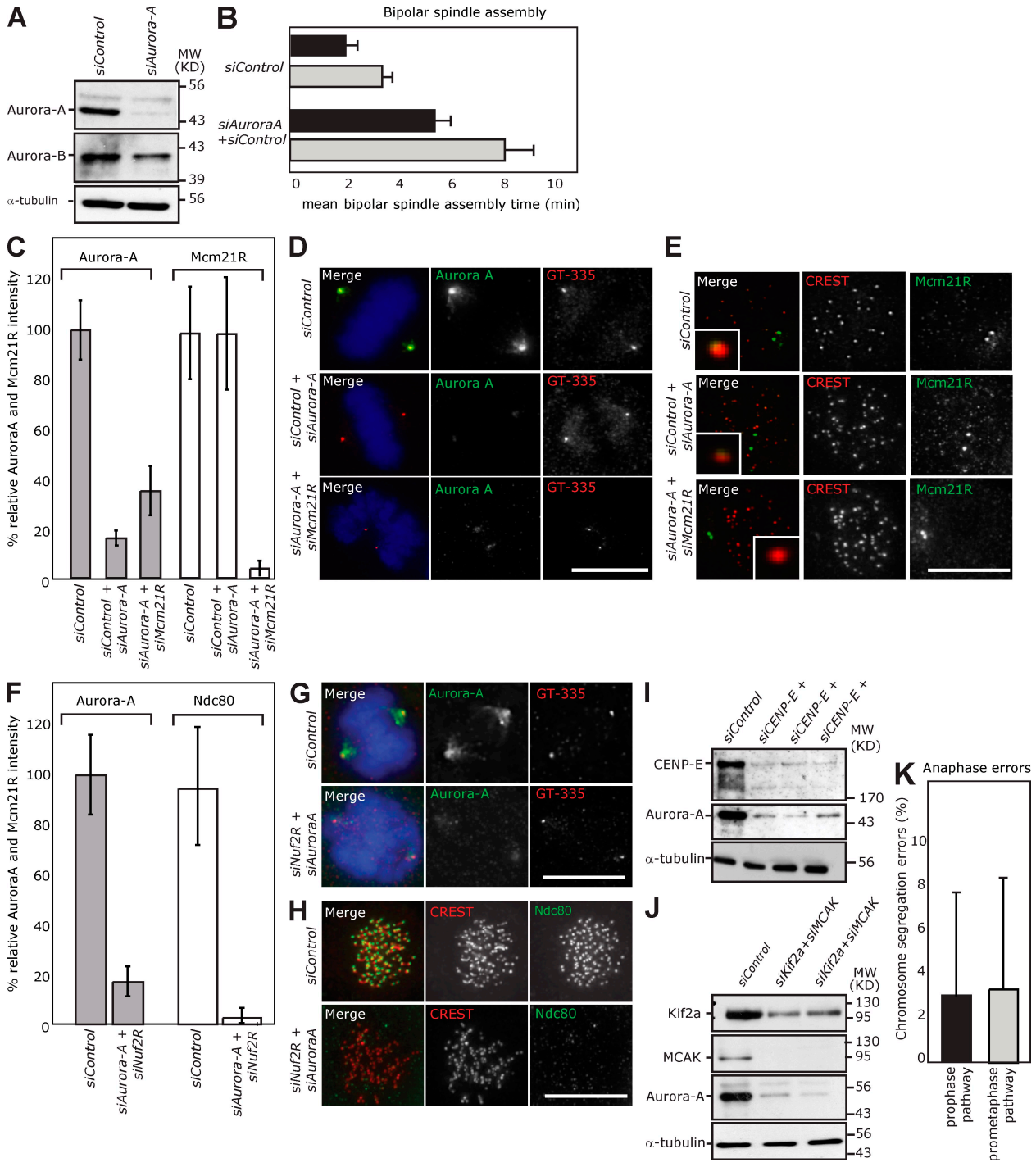

Figure S3. **Control experiments for siRNA depletions in Fig. 4 and demonstration that using the prophase or prometaphase pathways does not affect the accuracy of chromosome segregation.** (A) Immunofluorescence quantification of aurora A. Immunoblots of whole cell lysates from cells treated with *siControl* or *siaurora A* RNAs and probed with aurora A, aurora B or α-tubulin antibodies are shown. (B) Mean bipolar spindle assembly time in the prophase (black bars) or prometaphase (gray bars) pathway after depletion of aurora A ($n = 40$) or treatment with *siControl* RNA ($n = 73$). (C–E) Quantification of Mcm21R and aurora A depletion. Aurora A levels on centrosomes are based on the ratio of the aurora A signal with GT-335 signal (reference centrosome marker; the values are normalized to the ratio in *siControl*-treated cells). Representative images of cells transfected with siRNAs as indicated and stained with antibodies against aurora A (green), GT-335 antibodies (centrosome marker in red), and DAPI (DNA in blue), or Mcm21R (green), CREST (kinetochore marker in red), and DAPI (DNA in blue) are shown in D and E. Insets in E show higher magnification views of a single kinetochore. (F–H) Levels of aurora A and Ndc80 on kinetochores in cells stained with Ndc80 (reference marker for the NDC80 complex; note that Nuf2R depletion causes complete loss of Ndc80 protein from kinetochores; Merldi, P., V.M. Draviam, and P.K. Sorger. 2004. *Dev. Cell.* 7:45–60) or aurora A antibodies and CREST antisera (kinetochore marker) or GT-335 (as a reference for aurora A) after treatment with *siControl* or *siNuf2R + siaurora A* RNAs. Representative images are shown in G and H. (I) Validation of the aurora A and CENP-E depletions. Immunoblots of whole cell lysates from cells treated with siRNAs as indicated and probed with aurora A, CENP-E, or α-tubulin antibodies are shown. For functional experiments, the *siCENP-E + siaurora A* (2:1 combination) was used. (J) Validation of the aurora A, MCAK, and Kif2a depletions. Immunoblots of whole cell lysates treated with siRNAs as indicated and probed with Kif2a, MCAK, aurora A, or α-tubulin antibodies are shown. For functional experiments, the *siKif2a + siMCAK + siaurora A* (2:1:1 combination) was used. (K) Quantification of chromosome segregation errors (DNA bridges or lagging chromosomes after anaphase onset) for 70 wild-type HeLa cells in the prophase and prometaphase pathways. MW, molecular weight. Error bars represent SEM. Bars, 10 μm.

Published February 9, 2009

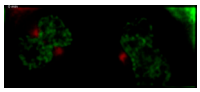

Video 1. **HeLa H2B-EGFP/α-tubulin–mRFP cells.** The video shows one cell following the prometaphase pathway and one following the prophase pathway. Frames are shown every 3 min, and the still images are shown in Fig. 1 B.

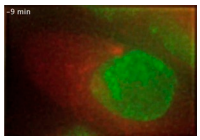

Video 2. **Mcm21R-depleted HeLa H2B-EGFP/α-tubulin–mRFP cell following the prophase pathway.** Frames are shown every 3 min, and the still images are shown in Fig. 4 E.

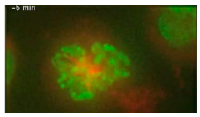

Video 3. **Mcm21R-depleted HeLa H2B-EGFP/α-tubulin–mRFP cell following the prometaphase pathway.** Frames are shown every 3 min, and the still images are shown in Fig. 4 F.

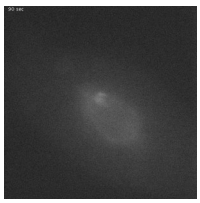

Video 4. **MT poleward flux after photoactivation of PA-GFP–α-tubulin in a control cell.** Frames are shown every 10 s, and the still images are shown in Fig. 2 A.

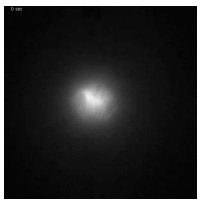

Video 5. **MT poleward flux after photoactivation of PA-GFP–α-tubulin in an MCAK + Kif2a–depleted cell.** Frames are shown every 10 s, and the still images are shown in Fig. 2 A.

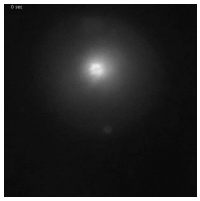

Video 6. **MT poleward flux after photoactivation of PA-GFP–α-tubulin in an Mcm21R-depleted cell.** Frames are shown every 10 s, and the still images are shown in Fig. 2 A.

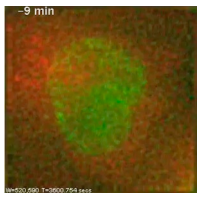

Video 7. **HeLa H2B-EGFP/α-tubulin–mRFP cells treated with *siCLASP1/2* in the prometaphase pathway.** Frames are shown every 3 min.

Published February 9, 2009

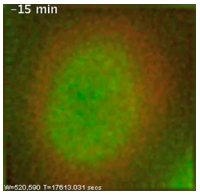

Video 8. **HeLa H2B-EGFP/α-tubulin–mRFP cells treated with *siMCAK/siKif2a/siaurora A* in the prometaphase pathway.** Frames are shown every 3 min, and the still images are shown in Fig. 4 B.

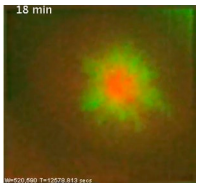

Video 9. ***siaurora* A/*siCENP-E*–treated HeLa H2B-EGFP/α-tubulin–mRFP cell in the prometaphase pathway.** Frames are shown every 3 min, and the still images are shown in Fig. 4 B.

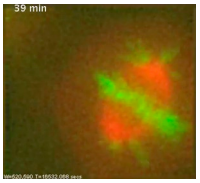

Video 10. ***siaurora* A/*siCENP-E*–treated HeLa H2B-EGFP/α-tubulin–mRFP cell in the prophase pathway.** Frames are shown every 3 min, and the still images are shown in Fig. 4 B.